Journal of Molecular Catalysis B: Enzymatic 61 (2009) 14–22

Contents lists available at ScienceDirect

Journal of Molecular Catalysis B: Enzymatic

journal homepage: www.elsevier.com/locate/molcatb

Multiple roles of mobile active center loops in the E1 component of the *Escherichia coli* pyruvate dehydrogenase complex—Linkage of protein dynamics to catalysis

Frank Jordan[a,*,1], Palaniappa Arjunan[b,2], Sachin Kale[a,2], Natalia S. Nemeria[a], William Furey[c,**,3]

[a] *Department of Chemistry, Rutgers University, Newark, NJ 07102, United States*
[b] *Biocrystallography Laboratory, Veterans Affairs Medical Center, Pittsburgh, PA 15240, United States*
[c] *Department of Pharmacology & Chemical Biology, University of Pittsburgh School of Medicine, Pittsburgh, PA 15261, United States*

ARTICLE INFO

Article history:
Available online 3 May 2009

Keywords:
Pyruvate dehydrogenase complex
Mobility of active center loop
Thiamin diphosphate
Electron spin resonance and loop mobility
^{19}F NMR probe of protein loop mobility

ABSTRACT

The region encompassing residues 401–413 on the E1 component of the pyruvate dehydrogenase multienzyme complex from *Escherichia coli* comprises a loop (the inner loop) which was not seen in the X-ray structure in the presence of thiamin diphosphate, the required cofactor for the enzyme. This loop is seen in the presence of a stable analogue of the pre-decarboxylation intermediate, the covalent adduct between the substrate analogue methyl acetylphosphonate and thiamin diphosphate, C2α-phosphonolactylthiamin diphosphate. It has been shown that the residue H407 and several other residues on this loop are required to reduce the mobility of the loop so electron density corresponding to it can be seen once the pre-decarboxylation intermediate is formed. Concomitantly, the loop encompassing residues 541–557 (the outer loop) appears to work in tandem with the inner loop and there is a hydrogen bond between the two loops ensuring their correlated motion. The inner loop was shown to: (a) sequester the active center from carboligase side reactions; (b) assist the interaction between the E1 and the E2 components, thereby affecting the overall reaction rate of the entire multienzyme complex; (c) control substrate access to the active center. Using viscosity effects on kinetics it was shown that formation of the pre-decarboxylation intermediate is specifically affected by loop movement. A cysteine-less variant was created for the E1 component, onto which cysteines were substituted at selected loop positions. Introducing an electron spin resonance spin label and an ^{19}F NMR label onto these engineered cysteines, the loop mobility was examined: (a) both methods suggested that in the absence of ligand, the loop exists in two conformations; (b) line-shape analysis of the NMR signal at different temperatures, enabled estimation of the rate constant for loop movement, and this rate constant was found to be of the same order of magnitude as the turnover number for the enzyme under the same conditions. Furthermore, this analysis gave important insights into rate-limiting thermal loop dynamics. Overall, the results suggest that the dynamic properties correlate with catalytic events on the E1 component of the pyruvate dehydrogenase complex.

1. Introduction

The *Escherichia coli* pyruvate dehydrogenase multienzyme complex (PDHc-ec) is comprised of three enzyme components: E1ec, E2ec and E3ec and catalyzes the oxidative decarboxylation of pyruvate according to Eq. (1) [1]:

$$CH_3COCOO^- + NAD^+ + CoASH \rightarrow CH_3COSCoA + CO_2 + NADH \quad (1)$$

The E1ec catalyzes thiamin diphosphate (ThDP)-dependent decarboxylation of pyruvate whose product reductively acetylates the lipoamide group of E2ec and then the acetyl group is used to generate acetylCoA on the E2ec component, to be used in the citric

Abbreviations: ThDP, thiamin diphosphate; LThDP, C2α-lactylthiamin diphosphate; PLThDP, C2α-phosphonolactylthiamin diphosphate; HEThDP, C2α-hydroxyethylthiamin diphosphate; MAP, methyl acetylphosphonate; PDHc, pyruvate dehydrogenase multienzyme complex; E1ec, E1 subunit of *E. coli* pyruvate dehydrogenase multienzyme complex; E2ec, *E. coli* dihydrolipoamide transacetylase; E3ec, *E. coli* dihydrolipoamide dehydrogenase; CD, circular dichroism; MALDI TOF/TOF, matrix-assisted laser desorption ionization time-of-flight/time-of-flight; FT ICR MS, Fourier-transform ion cyclotron resonance mass spectrometry; GC, gas chromatography; ΔG, Gibbs free energy change; ΔH, enthalpy change; ΔS, entropy change; ΔC_p, heat capacity change; TFA, trifluoroacetic acid; MM, Michaelis Menten complex; MTSL, (1-oxyl-2,2,5,5-tetramethylpyrrolidin-3-yl) methanethiosulfonate; *ee*, enantiomeric excess.

* Corresponding author. Tel.: +1 973 353 5470; fax: +1 973 353 1264.
** Corresponding author. Tel.: +1 412 683 9718.
E-mail addresses: frjordan@rutgers.edu (F. Jordan), fureyw@pitt.edu (W. Furey).
[1] Regarding biochemical aspects.
[2] These authors contributed equally to the work.
[3] Regarding structural issues.

1381-1177/$ – see front matter © 2009 Elsevier B.V. All rights reserved.
doi:10.1016/j.molcatb.2009.04.008

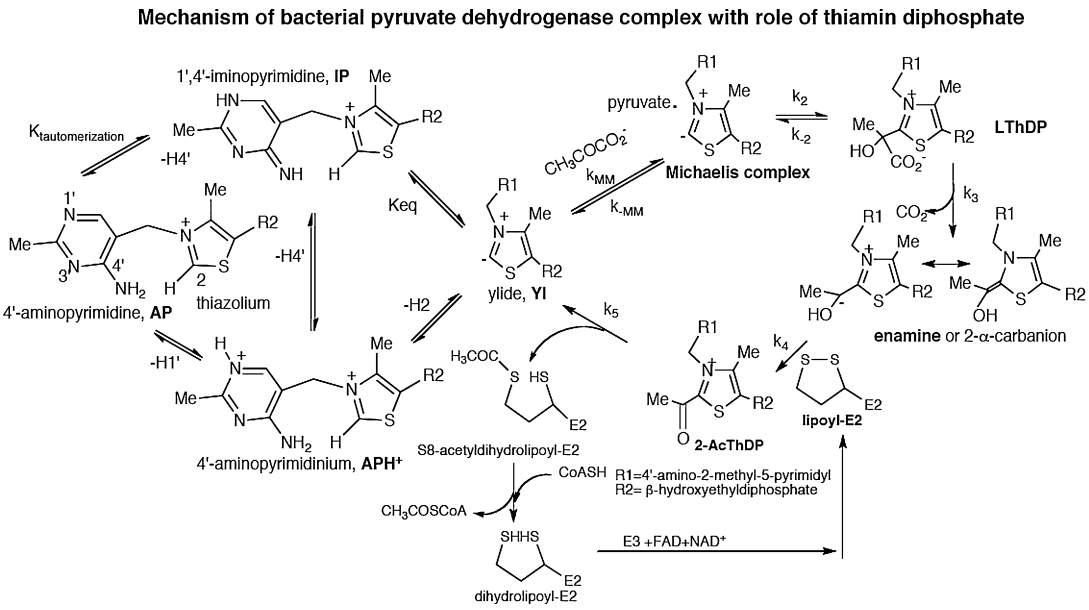

Scheme 1. Mechanism of bacterial pyruvate dehydrogenase complex with role of thiamin diphosphate.

acid cycle (Scheme 1). On the basis of a combination of site-directed mutagenesis and structural evidence, it became clear that there are some mobile loops of catalytic significance in the enzyme, loops which become organized when a substrate is bound to the active center ThDP. In view of these findings, it was of interest to attempt to determine the dynamics of these loops and to establish whether or not their dynamic properties correlate with any catalytic events. Below, we summarize this fascinating story; the results provide an additional example of a correlation of dynamics and catalysis on a ThDP-dependent enzyme, already reported on the E1 component of *Bacillus stearothermophilus* [29].

2. Structural evidence for the importance of mobile loops in catalysis

2.1. Identification of possible mobile loops and their likely implication in catalysis

The first crystal structure determination of an intact, dimeric, pyruvate dehydrogenase multienzyme complex E1ec was achieved in 2002 at 1.85 Å resolution [2], and revealed, along with the overall fold and active site, that three regions comprising a total of about 10% of each monomer (residues 1–55, 401–413, 541–557) were disordered. This was deduced from the facts that no interpretable electron density is observed in these regions, yet analysis of washed and re-dissolved crystals by mass spectrometry indicated these regions were indeed present and had not been excised by proteolysis. Knowledge that these regions, though disordered, had to be present in the crystal led to structural comparisons with known structures of other ThDP-dependent enzymes in an attempt to determine possible locations for some of these regions, at least during some transient steps in the catalytic mechanism. The most useful comparison was with the enzyme transketolase (TK) [3], that has low sequence homology with E1ec and catalyzes cleavage of the C–C bond of keto sugars and the subsequent transfer of a two-carbon unit to aldo sugars. But, unlike some other ThDP-dependent enzymes, TK has in common with E1ec the facts that these enzymes involve both donor and acceptor substrates, and they both assemble the three domains in each chain in the same order. Overall superposition of the E1ec and TK structures is shown in Fig. 1a, while the superimposed active site regions are shown in Fig. 1b. The TK magenta regions in Fig. 1b correspond to the disordered region (residues 401–413) in E1ec, and suggest that a similar position might be obtainable in E1ec during some point in the reaction, bringing additional reactive residues into the active site. Of particular interest is the reactive residue H263 in TK that corresponds to H407 in E1ec. This residue is highly conserved and positioned deep in the active site where it could conceivably interact with substrates or reaction intermediates.

An H407A mutation in E1ec was prepared and characterized to see if it affects catalysis [3]. The results were striking as this mutation only modestly affected catalysis through the pyruvate decarboxylation step in isolated E1ec (14% activity relative to parental E1ec), but profoundly inhibited the overall complex reaction by three orders of magnitude (0.15% activity compared to parental E1ec). This implies that H407 is crucial for post-decarboxylation steps in the reaction: it is likely that it is directly involved in reductive acetylation of lipoamide of the E2ec component, or indirectly involved by mediating E1ec–E2ec assembly interactions. Evidence was reported for the former by showing that in model reactions for the enamine, the dithiolane ring of lipoic acid was remarkably unreactive as an electrophile, until it was itself activated by another electrophile [4,5]. Dramatic rate accelerations were obtained only by methylating one of the two sulfur atoms, with the methylation serving as a substitute for protonation. Under those conditions formation of a tetrahedral intermediate at C2α was demonstrated between a sulfur of lipoamide and the C2α atom of the enamine. We thus proposed that H407 may be involved in protonation of lipoamide, thereby activating it toward reductive acetylation in the E1ec active site. We then pointed out that both the E1ec component and TK carry out ligation reactions, and TK is also faced with the problem of activating a very weak base (protonation of a carbonyl functional group). If H407 (and its counterpart H263 in TK) were required for such activation, it would explain the high conservation of this active site residue in both enzyme families.

2.2. Confirmation of loop mobility and the importance of H407 in the catalytic mechanism by high resolution structural analysis of a reaction intermediate analogue

As part of studies to elucidate details for the catalytic mechanism, E1ec crystals were obtained in complex with C2α-

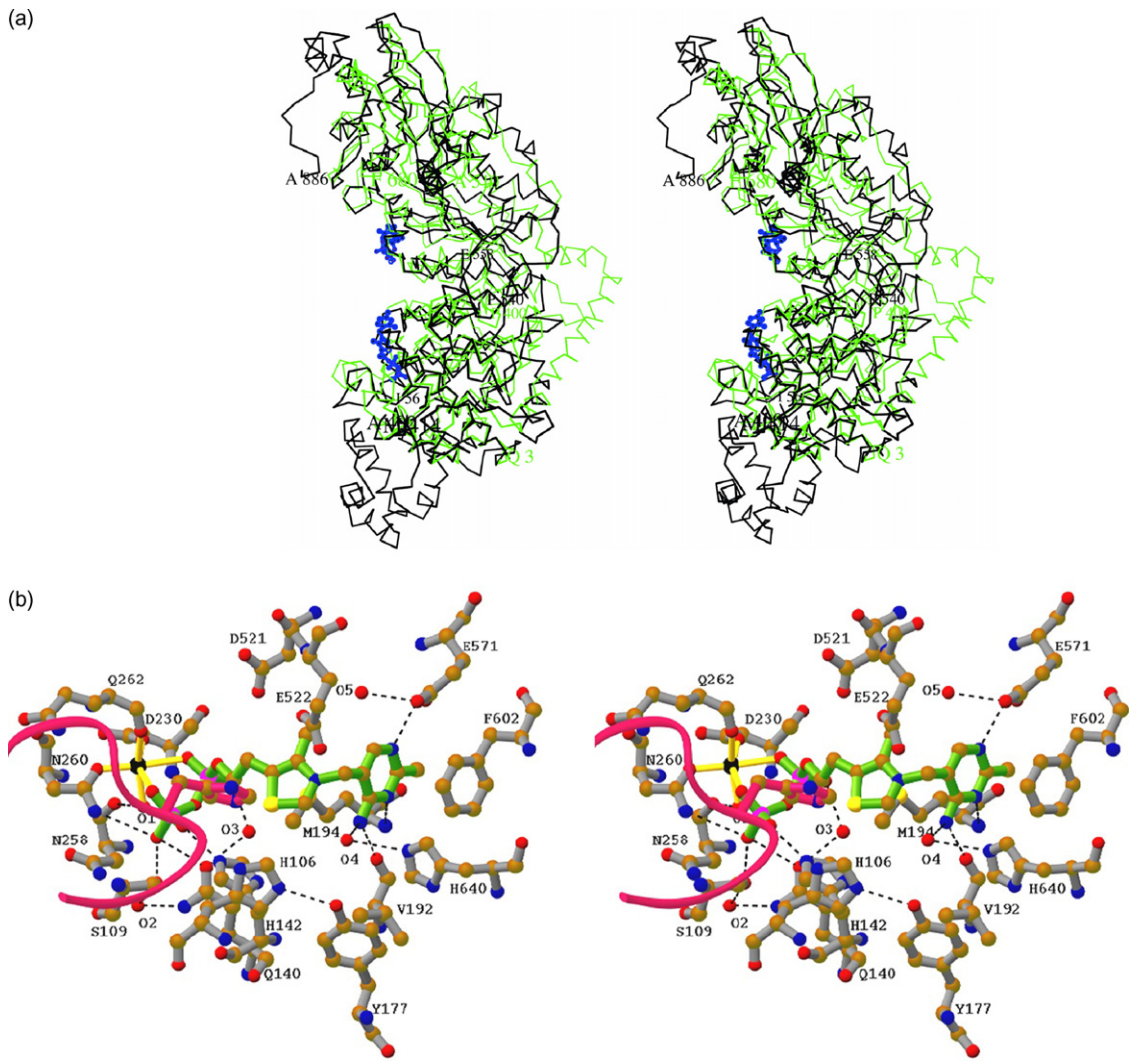

Fig. 1. (A) Stereo illustration of an *E. coli* PDHc E1 subunit superimposed on an *S. cerevisiae* TK subunit. Colors are green and black for the E1 and TK structures, respectively. The ThDP cofactors are shown in blue. (B) Stereo illustration of the active site environment in *E. coli* PDHc E1 with the TK structure superimposed. E1 residues numbered less than 471 are from the N-terminal of one subunit, and those greater than 470 are from the middle domain of the "other" subunit forming the active dimer. The main chain and histidine residue unobserved in E1 but present in TK are shown in magenta. The cofactor ThDP is shown in green. (For interpretation of the references to color in this figure legend, the reader is referred to the web version of the article.)

phosphonolactylthiamin diphosphate (PLThDP), the product of the reaction between the cofactor ThDP and methyl acetylphosphonate (MAP), where MAP is an analogue of the natural substrate pyruvate. The enzyme complex with PLThDP mimics the enzyme-bound, reactive pre-decarboxylation tetrahedral intermediate C2α-lactylThDP (LThDP; Scheme 1) [6], in terms of both structure and electrostatics. However, this complex differs from that formed with the true substrate in that the CO_2 group of pyruvate has been replaced with a PO_3 group, with one of the oxygen atoms methylated. The PLThDP complex has the advantage that it is stable since the C2α–PO_3Me bond is not cleaved, unlike the C2α–CO_2 bond with the natural substrate. The crystal structure of the PLThDP–E1ec complex has been determined at 2.1 Å resolution [7], and is crucial to confirming the mobility of loops during catalysis, as well as the need for H407.

The most surprising aspect of the PLThDP–E1ec structure is that unlike in the original structure, two of the previously disordered loops (residues 401–413 and 541–557) had become completely ordered. These two regions were found to interact with each other while completing the active site, with some of their residues forming direct contacts with the reaction intermediate analogue. Some of the newly ordered residues and a key interaction formed with the intermediate analogue are shown in Fig. 2. It is seen that H407 forms a direct hydrogen bond with one of the analogue's oxygen atoms. To determine the importance of this interaction, the crystal structure of the PLThDP complex with an H407A E1ec variant was also determined at 1.85 Å resolution [7]. In that case, although the PLThDP was totally ordered as before, the overall structure reverted back to the initial state with both loop regions totally disordered. Since the original, PLThDP–E1ec, and PLThDP–E1ec H407A structures are all isomorphous with no changes in packing contacts, the disorder-to-order transformation can only be attributed to the simultaneous presence of the reaction intermediate adduct and H407. This implies the hydrogen bond formed between H407 and the adduct is likely to be important. Another important aspect of the structural analysis with the PLThDP–E1ec complex is that with the two regions now ordered, the now completely lined active site channel leads directly to the enzyme surface (shown in Fig. 3). Some of the residues in the newly ordered regions form a new surface at the active site entrance, which is ideally situated to interact with the E2ec component of the multienzyme complex. All of the results strongly implicate the disorder-to-order transformation as being important in the catalytic mechanism, either by direct participation in the reaction or by facilitating favorable E1ec–E2ec interactions required

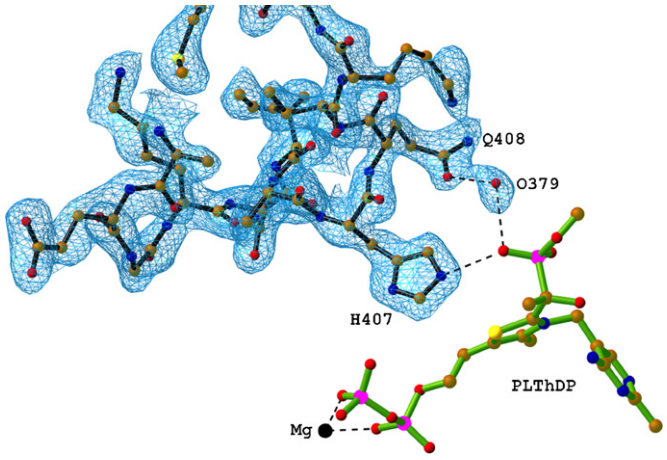

Fig. 2. 2Fo-Fc omit electron density map contoured at 1σ for part of the region that became ordered in the presence of PLThDP. The reaction intermediate analogue PLThDP is shown as a ball and stick figure. *Note*: the hydrogen bond between the analogue and His407.

for product/substrate channeling between enzymatic components within the complex. The results also indicated several interactions between residues within the mobile loop regions that may be important and are discussed below [8]. What was not known at the time was the frequency of the transition, i.e., whether it occurs once upon forming the first reaction intermediate and persists, or whether it occurs on each turnover.

3. Mechanistic importance of the E1ec inner mobile loop in catalysis

3.1. Site-directed mutagenesis results [8]

Substitution of charged residues to alanine in the inner loop (other than of His407) resulted in reduction of k_{cat} for the overall reaction of the complex by as much as 10-fold. This is a modest reduction and rules out any major roles of these residues in catalysis. The $K_{d\ ThDP}$ was unchanged in all charge-reversed variants as compared to E1ec. While there was only a modest threefold increase in $K_{m\ pyruvate}$, there was a significant reduction in $k_{cat}/K_{m\ pyruvate}$ for E401A and K403A indicating that substitution at these positions affected the rate of pre-decarboxylation steps. These observations could be the result of: (1) charges on these residues assisting directly substrate binding and specificity, or (2) disordering of the loop perhaps caused by neutralization of charges on these residues thus eliminating the stabilizing interactions. In contrast, the charge-reversed variants examined retained little activity (reduced k_{cat} as much as 177-fold) and could not be analyzed by steady-state kinetics. Instead, we assessed the effects by direct measurements of the apparent dissociation constant for the substrate analogue MAP ($K_{d\ MAP}$). The $K_{d\ MAP}$ values for charge-reversed variants E401K and K403E were 129- and 136-fold higher, respectively, than with E1ec, while the $K_{d\ MAP}$ values for E401A and K403A were only 9- and 12-fold higher, respectively. In K410E this value was reduced 7-fold but remained unchanged in K411E compared to E1ec. These observations indicate greatly reduced $K_{d\ MAP}$ (impaired covalent addition of substrate to ThDP) when charges are reversed, and suggest that charges on loop residues have an important role in this step, via modulation of loop dynamics. Not surprisingly, in H407A, shown to be essential for disorder to order transition of the loop [3], $K_{d\ MAP}$ increased 221-fold. We suggest that the hydrogen bond from H407 to PLThDP with the closed loop conformation is also present when substrate pyruvate binds to the coenzyme forming LThDP [7], and this interaction would thus stabilize this intermediate (discussed in Section 1.2).

Direct involvement of charged loop residues in substrate binding could also be ruled out since the value of $K_{d\ MAP}$ increased with a reduction in activity, and, responded dramatically to charge variations. The fractional increase in $K_{d\ MAP}$ in loop variants (as compared to H407A) could be due to impaired juxtaposition of H407 with respect to intermediate due to loop disorder, hence, H407 not only clamps down on the bound substrate, it is also directly responsible for stabilizing the LThDP form. This substrate induced 'clamping' or 'capping' action is reported in many enzymes whose catalysis is controlled by loop gating [see Ref. [30] for a review]. This is further supported by the observed stabilization of the otherwise transient MM complex in those loop variants in which the degree of loop disorder can be said to be at a maximum.

The N404A led to the greatest reduction in overall activity among the alanine-substituted variants and also greatly affected the $K_{d\ MAP}$ (33 μM) as expected, since N404 is within hydrogen bonding distance of, it interacts with the outer loop [7] and this interaction is essential for proper closure of this loop [9].

Thermodynamics of MAP binding to E1ec and its loop variants supported the above hypothesis. The van't Hoff's plot for E1ec was nonlinear in the accessible temperature range resulting in $\Delta C_p = -245.7$ cal mol^{-1} K^{-1}. ΔC_p has been related to the change in polar (ΔA_p) and non-polar (ΔA_{np}) surface area (Å^2), which accompanies binding [10].

$$\Delta C_p = 0.32\Delta A_{np} - 0.14\Delta A_p \quad (2)$$

Binding of MAP to E1ec yielded ΔA_{np} value of -646.28 Å^2 and ΔA_p value of -173.45 Å^2 indicating that binding is predominantly accompanied by burial of non-polar surface area. These are typical values reported for ligand binding processes coupled to folding events [10]. This observation is also consistent with the crystal structure, which shows the intermediate analogue PLThDP in the active site in the ordered conformation being surrounded by hydrophobic residues; these residues may not be juxtaposed in the disordered conformation, exposing these residues to solvent. In the absence of a crystal structure for the disordered conformation, we were unable to obtain a theoretical estimate of ΔA_{np} and ΔA_p during the disorder to order transition. The finding that with the inner loop variants ΔC_p is zero, suggests the absence of binding-coupled conformational changes upon MAP addition, and hence impaired ordering of the loop(s).

It was shown that the fractional reduction in E1 component-specific activity (measured by the external oxidizing agent 2,6-dichlorophenolindophenol, DCPIP) is always smaller than the fractional reduction in overall complex activity (measuring NADH production). *This is an indication of disruption in communication between the E1ec and E2ec components*. Disordering of the inner loop therefore affects the transfer of acetyl group from E1ec to the lipoamide on E2ec. Based on such observations and those from the structure of PLThDP–E1ec in which a new surface is formed in the active site channel as a result of loop ordering, it was proposed that this new surface facilitate E2ec-lipoyl domain binding and receiving lipoamide in the active center [7]. In H407A this newly ordered surface was not seen due to disorder of the loops and could explain the disruption of active site coupling in H407A.

To test the hypothesis that covalent substrate addition and reductive acetylation (active site coupling) are greatly impaired as a result of disorder in the loop caused by substitutions, the E401K variant was crystallized in the presence of PLThDP. Indeed, we found that both loops are disordered in both the ThDP–E401K and in the PLThDP–E401K complexes [8]; in the variants the presence of PLThDP in the active site is insufficient to form a strong hydrogen bond with H407 (present in the loops 401–413) for ordering this loop in the active site channel. Compared to the PLThDP–E1ec structure [7], there is no conformational rearrangement of active site residues in the PLThDP–E401K complex. Analysis

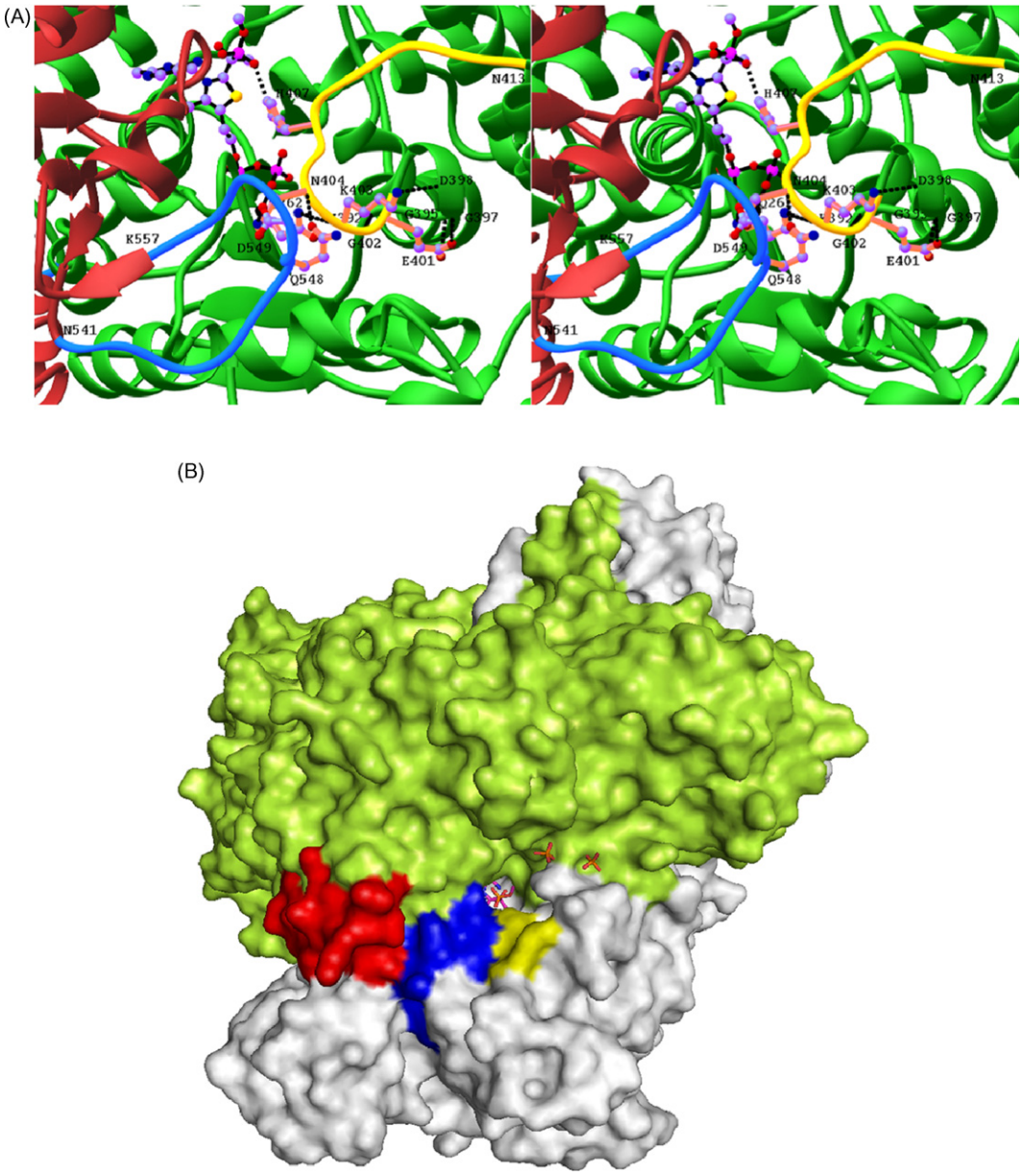

Fig. 3. Location of the inner loop on E1ec. (A) Stereo view of inner loop and intermediate (1′-4′ imino tautomer of PLThDP) hydrogen bonding in active site loops 401–413 (yellow) from subunit A (green) and 541–557 (blue) from subunit B (red) of E1ec. PLThDP (analogue of LThDP) is seen in the active site. Hydrogen bonding (···) between loops and between H407 and PLThDP can be seen. (B) Surface view of the E1ec showing active site channel and the positions of two loops [401–413 in blue from subunit α_{2a} (white) and 541–557 in red from subunit α_{2b} (green)]. The interaction of two loops creates a new surface leading to active site formed at the interface of two subunits [7]. The positively charged residues K410 and K411 lining the active site cavity can be seen in yellow. Intermediate analogue, in presence of which loops gets organized, can be seen deep inside active site cavity. Coordinates of PDB file 2G25 was used to create figure with the help of Pymol. (For interpretation of the references to color in this figure legend, the reader is referred to the web version of the article.)

of the PLThDP–E1ec structure revealed that residues present in the inner loop are involved in strong hydrogen bonding interactions with the residues present in loop region 392–400 [7], a loop region that is ordered in all E1ec structures, in the complexes with ThDP or PLThDP, and in the structures of different 401–413 loop variants. The inner loop forms several hydrogen bonds with this 392–400 loop, and these interactions also play a significant role for ordering the loops 401–413 in the active site channel.

3.2. Ordering of the inner loop protects the active center from 'carboligation' side reactions

Disruption of loop closure over the active center in loop-substituted variants would also mean impaired sequestering of active site chemistry from solvent. To test the plasticity of the active center, we used the carboligase side reactions as a diagnostic probe, reactions common with some ThDP-dependent decarboxylases. This is a reaction of the enamine with adventitious electrophiles competing with: (a) protonation in the non-oxidative decarboxylases, or (b) oxidizing agents in the oxidative decarboxylation reactions, such as with the lipoylE2. These electrophiles are typically the aldehyde product leading to acetoin and derivatives, or the 2-oxoacid starting material itself leading to acetolactate and derivatives. Certain active center substitutions on both E1ec [11] and the yeast pyruvate decarboxylase (YPDC [12]) have been shown to favor such carboligase side reactions over the principal product-forming reaction. According to NMR analysis, the molar ratio of acetolactate to acetoin is 1.25 when E1ec is incubated with excess

pyruvate. These data coupled with CD analysis of the above reaction revealed an approximately 10% *ee* of (*S*)-acetoin and a small *ee* of (*R*)-acetolactate, both detectible by their characteristic CD signals [(*S*)-acetoin gives a positive band with λ_{max} near 280 nm, while (*R*)-acetolactate gives rise to a negative band with λ_{max} at 301–302 nm [11]]. If active site loops do not sequester the intermediate due to disorder caused by substitutions, then we would expect this ratio to become larger than obtained with E1ec. Analysis of the carboligation products revealed that the molar ratio of acetolactate/acetoin varied inversely with activity, i.e., a lower the activity of variant, led to higher ratio of acetolactate relative to acetoin.

According to CD and chiral GC analysis, the H407A and H407C variants produced excess (*R*)-acetoin (negative CD band at 280 nm), while parental E1ec produced an excess of (*S*)-acetoin (~10% *ee*; positive CD band at 280 nm). This result suggests that the enamine intermediate changes its facial preference for the *re* face of acetaldehyde with these variants and the residue H407 also has an influence on the facial selectivity of the carboligase reaction. The carboligase product distribution and its stereochemical outcome are sensitive probes of access to the active center. As discussed in Section 1.1, the reactive residue H263 in TK corresponds to residue H407 in E1ec, and both of these residues interact with substrates/analogues in the active centers. Using a combination of chiral GC, CD and NMR, we have shown that this interaction on E1ec not only facilitates catalysis, but is also important in aligning incoming substrate vis-à-vis the active center ThDP, presumably facilitating formation of the near-attack conformation (NAC). We hypothesize that the dynamic inner loop also serves an important function in pre-organizing the active center for the substrate addition step, an essential prerequisite for an enzyme catalyzing multiple chemical steps requiring the stabilization of multiple transition states during catalysis [28]. Further studies are needed to provide additional support for this hypothesis.

Substitutions at different positions along the loop affected ordering of the loop and the magnitude of disorder induced is qualitatively mirrored by the carboligation product profile. Informatively, the major carboligation product of the K410A, K410E, K411A and K411E variants is (*S*)-acetoin with a small amount of racemic acetolactate. NMR analysis revealed that the molar ratio of acetoin to acetolactate was higher with the variants than with E1ec [the molar ratio of acetoin/acetolactate was 0.8 (E1ec), 1.20 (K410A), 1.45 (K410E), 1.05 (K411A) and 1.43 (K411E)] [8]. This suggests that, unlike with E1ec and other loop variants, with neutral and charge-reversed substitution at K410 and K411, the second pyruvate cannot readily access the active center to add to the enamine to generate acetolactate. Thus the reactive enamine reacts more frequently with acetaldehyde generated in the active center in the absence of oxidizing agent; the positive charge at K411 and K410 is needed to assist entry of the second molecule of pyruvate forming acetolactate, and presumably of the first one as well. Binding curves of ThDP to apo K410 and K411 variants yielded Hill coefficients (n_H), which indicated that these substitutions induced cooperativity in ThDP binding, yet, the $K_{d\ ThDP}$ values remained unchanged in the variants. Therefore, the positive charges lining the active site entrance help entry of ThDP independently in both active sites of the dimer, but, in the absence of these charges, structural changes in the active site (composed of residues from both subunits) that occur upon binding of ThDP in one site must precede binding the second ThDP in the second active site [13]. These structural changes presumably propagate to the second active site and prepare it for binding the second ThDP.

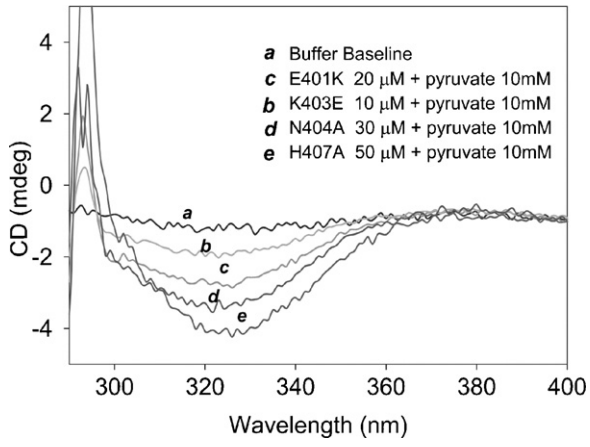

Fig. 4. Stabilization of transient Michaelis complex with pyruvate in low activity loop variants. Representative trace of each variant at a particular active site concentration is shown. In actual titration intensity of negative peak (centered at 327 nm) was proportional to active site concentration for all the variants in the figure.

3.3. Evidence for impaired communication between the E1ec and E2ec components when the loops are unorganized

We had shown earlier that MALDI-TOF and MALDI-TOF-TOF MS methods provide a clear measure of the effectiveness of acetyl transfer (reductive acetylation) between the E1ec and E2ec components. The rate of reductive acetylation of E2ec and of independently expressed lipoyl domain was affected in several loop variants. The independently expressed lipoyl domain was fully acetylated after 1 min of incubation with E1ec and pyruvate. However, the loop variants with low activity exhibited slower reductive acetylation (E401K, K403E and N404); unacetylated lipoyl domain could be detected even after 30 min of incubation, suggesting a dramatic reduction in subunit communication, as reported for H407A earlier.

3.4. Evidence for impaired rates of formation of the pre-decarboxylation intermediate and the surprising stability of the Michaelis Menten complex when loops are unorganized

Earlier, we had reported that addition of excess pyruvate to a solution of E1ec complexed with ThDP and pre-incubated with 0.2 mM pyruvate reveals the presence of a transient MM complex, characterized by a broad negative CD band centered at 327 nm [14]. We hypothesized that under these conditions the MM complex was stabilized by the slow turnover of the substrate due to the presence of a dead-end intermediate, C2α-hydroxyethylThDP (HEThDP), in one of the two active sites. In the absence of pre-incubation with 0.20 mM pyruvate, the turnover is very fast and no MM complex could be detected. With the very low activity inner loop variants (E401K, K403E, N404A and H407A) the MM complex could be detected under both conditions, i.e., with or without pre-incubation with 0.20 mM pyruvate (Fig. 4). Based on the crystal structure results for E401K, as well as kinetics and CD studies of loop variants, we concluded that the MM complex in E401K, K403E, N404A and H407A is stabilized by a dramatic reduction in the rate of chemical transformation to LThDP as a consequence of the disordering of the loops.

4. Dynamic consequences of E1ec inner loop substitutions [9,15]

According to the previous summary, the dynamic behavior of the active center inner loop in E1ec is critical for catalytic functions starting from a pre-decarboxylation event and culminating in transfer of the acetyl moiety to the E2ec component (i.e., inter-component communication) [8]. The disorder-order transformation in E1ec modulated by interaction of H407 with PLThDP

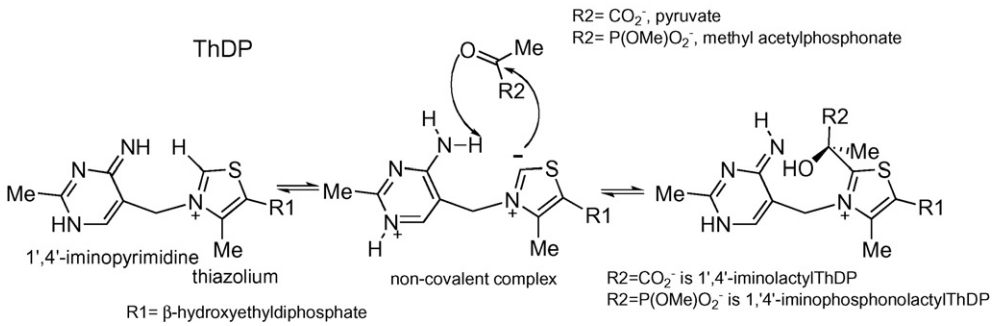

Scheme 2. Mechanism of formation of 1′,4′-iminolactyl ThDP and 1′,4′-iminophosphonolactyl ThDP as a result of covalent addition of substrate pyruvate and substrate analogue methyl acetylphosphonate (MAP), respectively to enzyme-bound ThDP.

acts as a 'feed-forward' switch by preparing the active site for the next step, receiving the lipoamide group of the E2ec component [7]. These observations suggested that the dynamics of the E1ec active center loops may be correlated to substrate turnover. Correlated biological processes of considerable interest such as ligand binding, catalysis and conformational transitions, occur on timescales ranging from picosecond to days and the conformational transition is often coupled to ligand binding and catalysis [16–18]. To quantify inner loop dynamics, we used site-specific labeling (SSL) of a cysteine-free E1ec variant (E1ec$_{-C6}$; replacing 6 cysteines/monomer) onto which single cysteines could be substituted at any desired position.

4.1. Loop dynamics influences covalent addition of the substrate to ThDP

Experiments were carried out to identify which microscopic step(s) in Scheme 1 respond to loop dynamics, using our assignment of a negative CD band centered near 320–330 nm to (a) the 4′-aminopyrimidine tautomer of ThDP (AP form) or (b) the Michaelis Menten (MM) complex formed either with substrate [19] or substrate analogue MAP [19,20]. Addition of pyruvate to the E401K loop variant under a variety of conditions produced the negative CD band corresponding to MM, stabilized as a result of very slow catalysis caused by impaired loop dynamics [8]. The MM was fully formed in E1ec and E401K, within the dead time (1 ms) of the stopped-flow CD instrument. However, formation of PLThDP from MAP (Scheme 2) on E1ec ($k_1^{obs} = 3.6 \pm 0.2\,s^{-1}$ and $k_2^{obs} = 0.35 \pm 0.06\,s^{-1}$) was slower than MM formation and significantly slower in E401K ($k_1^{obs} = 0.37 \pm 0.05\,s^{-1}$ and $k_2^{obs} = 0.04 \pm 0.01\,s^{-1}$). Hence, formation of C–C covalent bond (k_2 in Scheme 1), and not formation of MM (k_{MM}), is the rate-limiting pre-decarboxylation step, and loop dynamics greatly influences covalent addition of substrate to the enzyme-bound ThDP.

4.2. Viscosity dependent kinetics supports correlation of catalysis and loop dynamics

Variation of k_{cat}^0/k_{cat} [the ratio of the k_{cat}^0 measured in buffer to that measured in the presence of the viscogen (k_{cat})] with viscosity (η in E1ec gave a linear plot (slope = 0.06 ± 0.04) at low viscosity, but at higher viscosity the plot deviated from linearity. In contrast, such a plot for E401K was linear and displayed a much larger slope (0.8 ± 0.1). Consistent with this observation, similar values are observed for k_{cat} for pyruvate ($3.2 \pm 0.3\,s^{-1}$) and the rate of formation of PLThDP ($k_1^{obs} = 3.6 \pm 0.2\,s^{-1}$) at $\eta = 1.0$ in E1ec. Since formation of MM (k_{MM}), a step preceding LThDP formation, is not rate limiting for either E1ec or E401K [15], the lower catalytic rates (i.e., higher slopes) in the variants strongly suggest impaired catalysis due to loop disorder (i.e., impaired loop dynamics). That the nonlinear plot observed with E1ec reflect changes in loop dynamics as a result of increasing medium resistance, rather than a change in rate-determining step, was suggested by direct measurement of the rate of pre-decarboxylation steps in E1ec at $\eta = 5.3$. The MM was again fully formed within the mixing time of instrument (1 ms, unchanged at higher η); however, the rate of formation of PLThDP ($k_1^{obs} = 0.96 \pm 0.23\,s^{-1}$) was similar to k_{cat} ($1.0 \pm 0.3\,s^{-1}$) measured at $\eta = 5.3$. With E401K the $k_1^{obs} = 0.067 \pm 0.01\,s^{-1}$ was again similar to $k_{cat} = 0.07 \pm 0.01$ at $\eta = 5.3$. The results affirmed that the rate determining step is unchanged with increasing viscosity, and the nonlinear kinetics with increasing viscosity in E1ec reflect progressive impairment of loop dynamics and associated catalysis. Substitution at the highly conserved residue E571 to alanine served as a low activity control, showing that the observed viscosity effects on catalysis of E1ec and variants could be attributed to dynamic modulation of catalysis.

4.3. EPR studies reveal a dynamic equilibrium of conformations of the inner active site loop

The EPR spectrum of a nitroxide spin label inserted at position Q408C (Q408C–MTSL) revealed the presence of two components in the un-liganded enzyme at room temperature; an intrinsic component that is mobile with a rotational correlation time (τ_R) of 1.3 ns comprising 25%, and an immobile component ($\tau_R = 5.4$ ns) of 75%. Upon addition of MAP to form PLThDP, the τ_R for the mobile component remained the same but increased dramatically to 8.3 ns for the immobile component. Similar results were obtained for K411C–MTSL (K411C derivatized with MTSL), but, the contribution from the mobile component was very small and the spectra did not require simulation with a two-component model. A single-component simulation of the K411C–MTSL spectra showed an approximately 214% increase in the τ_R, indicating a dramatic reduction in the mobility of the probe on MAP addition. Compared to Q408C–MTSL, the τ_Rs for K411C–MTSL are fast; presumably the mobility of the probe in the presence and absence of MAP is faster in K411C–MTSL. Since K411 is located at the hinge of the loop, the probe could move more freely than at Q408, yet addition of substrate analogue gave a measurable change.

We have now shown on E1ec that the disordered active center loops become ordered on formation of PLThDP from MAP [7]. This ordered conformation could be associated with a closed one since it protects the active site from solvent, in contrast to a disordered (or open) conformation, in which the enamine reacts with excess pyruvate in the 'carboligation' side reaction [6]. Also, since the fraction of immobile component increased with concomitant decrease in the fraction of mobile component (their respective τ_R values showing reciprocal changes), we hypothesized that these components might represent two environments encountered by the probe reflecting different conformations. Consequently, changes in the

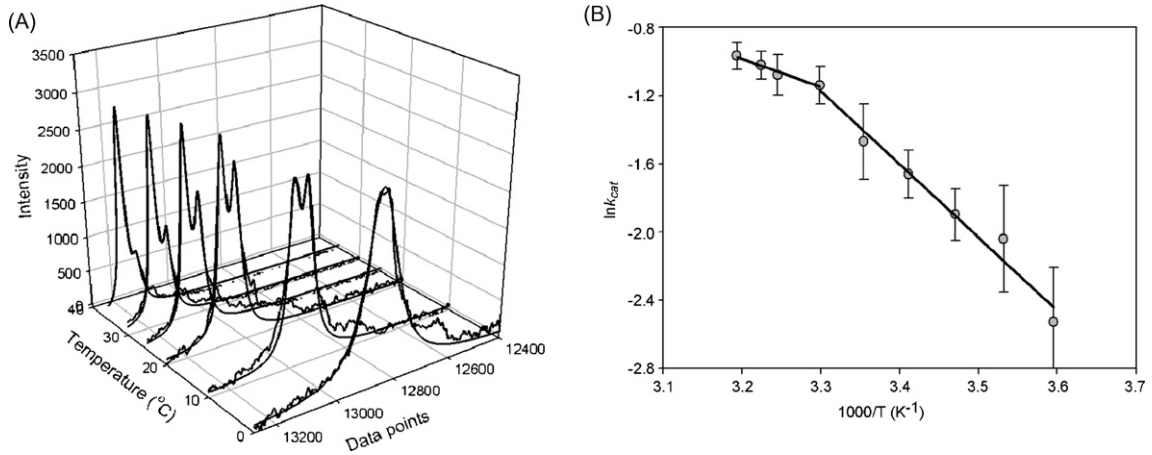

Fig. 5. (A) Lineshape simulations for un-liganded K411C labeled with TFA. The smooth line is a simulated spectrum. Data was simulated using WinDNMR-Pro assuming two state 'open × close' transitions. While linewidth and resonance frequency were kept constant the relative population of each state, baseline intensity and the exchange rates between states were allowed to vary. (B) Effect of temperature on the k_{cat} of K411C-TFA. The data are means ± SE from at least three measurements.

EPR spectra resulting from addition of MAP were assigned to a change in the ratio of open to closed states of the mobile loops. It was concluded that the loops exist in an equilibrium of open and closed states in the un-liganded state and the population shifts to a preponderance of the closed state on binding of the substrate analogue to produce PLThDP. We further hypothesized that similar changes would occur on binding of the substrate pyruvate in place of MAP.

4.4. ^{19}F NMR studies provide a quantitative estimate of the rate of active site loop fluctuations

To obtain dynamic information on a slower time scale than that afforded by the X-band EPR experiments, ^{19}F NMR experiments were carried out. The initial ^{19}F NMR studies confirmed the conclusions from EPR studies. The ^{19}F spectra of K411C-TFA (K411C derivatized with 1-bromo-3,3,3-trifluoroacetone) showed two distinct and unequally populated resonances at −8.993 ppm and −9.106 ppm, respectively. On addition of MAP, the resonance at −8.993 disappeared and the one at −9.106 became more intense, and the two were assigned to the closed and open conformations of the loop, respectively, consistent with the EPR observations. As the same resonances are also present in the un-liganded state (see below), the ligand-induced changes in chemical shift can be attributed to environmental changes around the probe rather than directly to the presence of ligand. As with the EPR results, the two resonances corresponding to open and closed conformations in K411C-TFA are not very well resolved because of the position of the probe. Nevertheless, two distinct states of a singly labeled enzyme could still be detected, impressive in view of the mass of the dimer (∼200 kDa).

In the un-liganded population, the conformational equilibria exhibited strong temperature dependence (Fig. 5) and resemble chemical exchange type effects [21], enabling estimation of exchange rates ($k_{ex} = k_{AB} + k_{BA}$) by line shape simulations. At all accessible temperatures, the line shape simulations yielded an exchange rate constant of <1.0 s^{-1}, very similar in order of magnitude to the observed k_{cat} of the K411C-TFA (k_{cat} = 0.38 s^{-1} according to E1-component-specific assay at 30 °C), and suggesting a *quantitative correlation of loop dynamics and catalysis in E1ec*. This is consistent with the variation of k_{cat} values for K411C-TFA with temperature (Fig. 5B) and strongly supports the quantitative correlation. We concluded that dynamics of active center loops may control a rate-limiting catalytic step consistent with stopped flow CD and viscosity data.

The ratio of open to closed populations exhibited remarkable temperature dependence. While low temperatures favor equal populations of the open and closed conformations, the open conformation predominates at higher temperatures.

4.5. Temperature dependent conformational equilibrium is also present in E1ec

To demonstrate that the conformational equilibrium of the inner loop observed with EPR and NMR studies is not an artifact of cysteine substitution, reintroduction of a cysteine, or of the introduction of covalent probes, we measured changes in enthalpy (ΔH_{obs}) on MAP binding as a function of temperature, using isothermal titration calorimetry (ITC) to characterize the conformational changes that accompany a binding event [22]. At lower temperatures (<25 °C), the ΔH_{obs} varied linearly with temperature, resulting in very low value of ΔC_{pobs}, however, above 25 °C there was a marked deviation from linearity. This temperature dependence of ΔH_{obs} and the resultant increase in negative ΔC_{pobs} is a hallmark of a process in which ligand binding is coupled to a conformational change [22], and is a thermodynamic signature of a pre-existing conformational equilibrium in the un-liganded enzyme [23–26]. Thus, the conformational equilibrium observed by EPR and NMR, and the step transition in population ratio in favor of the open (disordered) conformation at higher temperature (>25 °C) (according to deconvolution of the NMR signal, and reflected here by the ΔH_{conf} term), that were observed in cysteine-free and site specifically labeled E1ec used for these studies, are also present in the unsubstituted E1ec.

The mechanism of this process can be interpreted using the following assumptions typical of ligand-binding processes: (i) the association of MAP and E1ec comprises a rigid-body binding interaction and an intramolecular conformational change; (ii) the enthalpy and heat capacity of binding are negative ($\Delta H_{bind} < 0$ and $\Delta C_{pbind} < 0$); (iii) the enthalpy and heat capacity for the conformational transition are also negative ($\Delta H_{conf} < 0$ and $\Delta C_{pconf} < 0$), as if the binding induced conformational change caused burial of a hydrophobic binding pocket. The observed free energy of binding (ΔG_{obs}) was found to be entropically driven over the entire temperature range, likely due to changes in solvation [10], consistent with the observations and assumptions.

Binding of MAP to E1ec gave rise to striking isotherms. While at temperatures <30 °C the binding isotherm suggested two identical binding sites for the dimer, the affinities at the two sites differed sharply above 30 °C. The two distinct sites generated

at elevated temperatures bind MAP with 100-fold difference in affinity (K_{d1} = 0.03 μM and K_{d2} = 3.0 μM), as a result of difference in free energy of binding ($\Delta G^1_{obs} - \Delta G^2_{obs} = -2.84$ kcal/mol). This difference emanates entirely from the entropy change ($T\Delta S^2_{obs} - T\Delta S^1_{obs} = 3.94$ kcal/mol) and opposes the enthalpically favored binding of the second ligand. Therefore, the apparent negative cooperativity induced at higher temperature is entropically driven in its entirety.

As suggested by this study, formation of LThDP (k_2 in Scheme 1) is the rate-limiting step in E1ec catalysis due to its control by loop dynamics. Presumably, at higher temperatures, due to an increase in the rate of loop fluctuations (sharpening of NMR peak at 35 °C), k_2 increases, and, as a result the downstream chemical steps, particularly reductive acetylation of E2ec, could become rate limiting. Since cooperativity is a mechanism to sharpen or dampen the responsiveness of a system in response to a stimulus [27], we speculate that the negative cooperativity induced in E1ec at higher temperature might act as a regulatory switch to down-regulate the covalent substrate addition (k_2). This may assist the enzyme to proceed to reductive acetyl transfer to E2ec, before a second molecule of pyruvate can trap the enamine in the carboligase side reaction.

In the crystal structures of E1ec loop variants studied to date both loops are seen disordered even when the only stabilizing interactions that are disrupted by the substitutions are between the inner loop and the protein (E401K and K403E) [8] or between the inner loop and intermediate analogue (H407A) [7], rather than between two loops. Therefore, the dynamics of the two active center loops appear to be concerted, they work in tandem, leading us to speculate that our observations on inner loop dynamics would apply to the outer loop as well.

5. Conclusions

We have demonstrated that disorder to order transformation of the inner active center dynamic loop of E1ec modulates steps through LThDP formation. Ordering of loops also facilitates E1ec to E2ec active center communication, presumably by acting as a recognition site for the E2ec lipoyl domain, and acts as a regulatory switch for the next committed step in E1ec catalysis. The charged residues assist in loop dynamics, in sequestering the active site from carboligation side reactions and in substrate utilization. The results also revealed that the N404 residue is important for catalysis, subunit communication and it interacts with the outer loop and thus might control outer loop dynamics (possibly independently from the inner loop).

Our observations suggest efficient coupling of catalysis with dynamics, which appears to lower the transition state of covalent addition of substrate to ThDP by a combination of enthalpic and entropic components. As with many dimeric enzymes that use allosteric communication to regulate catalysis, E1ec uses negative cooperativity to regulate catalysis in the entire complex, but unusually, this regulation is entirely entropically driven. Our results suggest a conformational equilibrium in the un-liganded state of E1ec, also suggested by very different pre-steady-state kinetic experiments for YPDC [28]. Whether this is a common feature of ThDP-dependent decarboxylases necessitates further evaluation.

Acknowledgements

Supported by NIH GM 050380 (FJ) and NIH GM 061791 (WF).

References

[1] L.J. Reed, Acc. Chem. Res. 7 (1974) 40–47.
[2] P. Arjunan, N. Nemeria, A. Brunskill, K. Chandrasekhar, M. Sax, Y. Yan, F. Jordan, J. Guest, W. Furey, Biochemistry 41 (2002) 5213–5221.
[3] N. Nemeria, P. Arjunan, A. Brunskill, F. Sheibani, W. Wei, Y. Yan, S. Zhang, F. Jordan, W. Furey, Biochemistry 41 (2002) 15459–15467.
[4] C. Chiu, A. Chung, G. Barletta, F. Jordan, J. Am. Chem. Soc. 118 (1996) 11026–11029.
[5] K. Pan, F. Jordan, Biochemistry 37 (1998) 1357–1364.
[6] S. Zhang, M. Liu, Y. Yan, Z. Zhang, F. Jordan, J. Biol. Chem. 279 (2004) 54312–54318.
[7] P. Arjunan, M. Sax, A. Brunskill, K. Chandrasekhar, N. Nemeria, S. Zhang, F. Jordan, W. Furey, J. Biol. Chem. 281 (2006) 15296–15303.
[8] S. Kale, P. Arjunan, W. Furey, F. Jordan, J. Biol. Chem. 282 (2007) 28106–28116.
[9] S. Kale, PhD Dissertation, Rutgers University, Graduate Faculty at Newark, 2007.
[10] R.S. Spolar, M.T. Record, Science 263 (1994) 777–784.
[11] N. Nemeria, K. Tittmann, E. Joseph, L. Zhou, M. Vazquez-Coll, P. Arjunan, G. Hübner, W. Furey, F. Jordan, J. Biol. Chem. 280 (2005) 21473–21482.
[12] E.A. Sergienko, F. Jordan, Biochemistry 40 (2001) 7369–7381.
[13] C. Krishnamoorthy, P. Arjunan, M. Sax, N. Nemeria, F. Jordan, W. Furey, Acta Crystallogr. D62 (2006) 1382–1386.
[14] N. Nemeria, A. Baykal, E. Joseph, S. Zhang, Y. Yan, W. Furey, F. Jordan, Biochemistry 43 (2004) 6565–6575.
[15] S. Kale, G. Ulas, J. Song, G.W. Brudvig, W. Furey, F. Jordan, Proc. Natl. Acad. Sci. U.S.A. 105 (2008) 1158–1163.
[16] D. Kern, E.Z. Eisenmesser, M. Wolf-Watz, in: T.L. James (Ed.), Methods in Enzymology, Academic Press, 2005, pp. 507–524.
[17] A.G. Palmer, Chem. Rev. 104 (2004) 3623–3640.
[18] A. Mittermaier, L.E. Kay, Science 312 (2006) 224–228.
[19] N. Nemeria, L.G. Korotchkina, M.J. McLeish, G.L. Kenyon, M.S. Patel, F. Jordan, Biochemistry 46 (2007) 10739–10744.
[20] N. Nemeria, S. Chakraborty, A. Baykal, L.G. Korotchkina, M.S. Patel, F. Jordan, Proc. Natl. Acad. Sci. U.S.A. 104 (2007) 78–82.
[21] S. Rozovsky, G. Jogl, L. Tong, A.E. McDermott, J. Mol. Biol. 310 (2001) 271–280.
[22] M.J. Cliff, M.A. Williams, J. Brooke-Smith, D. Barford, J.E. Ladbury, J. Mol. Biol. 346 (2005) 717–732.
[23] R.A. Grucza, K. Futterer, A.C. Chan, G. Waksman, Biochemistry 38 (1999) 5024–5033.
[24] S. Kumaran, R.A. Grucza, G. Waksman, Proc. Natl. Acad. Sci. U.S.A. 100 (2003) 14828–14833.
[25] F.J. Bruzzese, P.R. Connelly, Biochemistry 36 (1997) 10428–10438.
[26] D. Keramisanou, N. Biris, I. Gelis, G. Sianidis, S. Karamanou, A. Economou, C.G. Kalodimos, Nat. Struct. Mol. Biol. 13 (2006) 594–602.
[27] D.E. Koshland, Curr. Opin. Struct. Biol. 6 (1996) 757–761.
[28] E.A. Sergienko, F. Jordan, Biochemistry 41 (2002) 3952–3967.
[29] R.A. Frank, C.M. Titman, J.V. Pratap, B.F. Luisi, R.N. Perham, Science 306 (2004) 818–820.
[30] S.J. Benkovic, S. Hammes-Schiffer, Science 301 (2003) 1196–1202.